Complexes Containing Heteronuclear Quadruple Bonds. Preparation and Characterization of α-Mo$\equiv$WCl$_4$(L-L)$_2$ (L-L = dppe, dmpe) and β-Mo$\equiv$WCl$_4$(L-L)$_2$ (L-L = dppm, dmpm, dppe)

F. A. Cotton* and Chris A. James†

Department of Chemistry and Laboratory for Molecular Structure and Bonding, Texas A&M University, College Station, Texas 77843-3255

Received April 21, 1992

The quadruply bonded heterobimetallic complexes Mo$\equiv$WCl$_4$(μ-dppm)$_2$·2THF·C$_6$H$_6$ (**1**), β-Mo$\equiv$WCl$_4$(μ-dppe)$_2$ (**2**), α-Mo$\equiv$WCl$_4$(dppe)$_2$ (**5**), Mo$\equiv$WCl$_4$(μ-dmpm)$_2$ (**3**), and α-Mo$\equiv$WCl$_4$(dmpe)$_2$·4CH$_2$Cl$_2$ (**4**) are formed in the reactions between Mo$\equiv$WCl$_4$(PMePh$_2$)$_4$ and bis(diphenylphosphino)methane (dppm), bis(diphenylphosphino)ethane (dppe), bis(dimethylphosphino)methane (dmpm), or bis(dimethylphosphino)ethane (dmpe), respectively. These complexes are the first examples of heteronuclear quadruply bonded complexes of the form M$\equiv$M′Cl$_4$(L-L)$_2$, where L-L groups are bidentate phosphines. Complexes designated α have chelating diphosphine ligands and complexes designated β have bridging diphosphine ligands. Complexes **1** and **2** cocrystallize with small amounts of Mo$\equiv$MoCl$_4$(μ-dppm)$_2$ or α-Mo$\equiv$MoCl$_4$(dppe)$_2$ forming solid solutions. The apparent Mo–W distances are 2.2110 (7) Å for Mo$\equiv$WCl$_4$(μ-dppm)$_2$ and 2.234 (1) Å for β-Mo$\equiv$WCl$_4$(μ-dppe)$_2$. Complexes **3** and **4** are free from contamination by their dimolybdenum analogs, and the Mo–W distances are 2.193 (2) Å for Mo$\equiv$WCl$_4$(μ-dmpm)$_2$ and 2.243 (1) Å for α-Mo$\equiv$WCl$_4$(dmpe)$_2$. In addition to the structural data for these complexes, each has been fully characterized using ^{31}P{^{1}H} NMR and ^{1}H NMR spectroscopy. Complexes **1–5** all have methylene or ethylene protons located at positions that allow the calculation of the diamagnetic anisotropy of the Mo$\equiv$W bond from the ^{1}H NMR chemical shift data. The crystal structures of **1**, **2**, and **4** are fully described. Crystallographic data for these compounds are as follows: **1**, $P2_1/c$ with a = 21.562 (3) Å, b = 14.567 (4) Å, c = 22.063 (4) Å, β = 118.82 (1)°, V = 6071 (2) Å^3, Z = 4; **2**, $P2_1/n$ with a = 23.099 (4) Å, b = 13.284 (1) Å, c = 16.765 (3) Å, β = 107.45 (2)°, V = 4894 (2) Å^3, and Z = 4; **4**, $P2_1/c$ with a = 10.422 (6) Å, b = 16.707 (6) Å, c = 11.406 (8) Å, β = 111.87 (6)°, V = 1843 (2) Å^3, and Z = 2.

Introduction

Of the thousands of compounds that contain M–M multiple bonds, of which several hundred have been structurally characterized, only about 1% contain heteronuclear bonds. Of these only ten[1-3] have been structurally characterized by X-ray crystallography. As with the homonuclear species, the heteronuclear multiple bonds need not be supported by bridging ligands, although some are. Those which were supported by carboxyl and 2-hydroxypyridinate ligands were the first to be studied, and it was found that the M$\equiv$M′ bonds were all shorter than the average of the corresponding M$\equiv$M and M′$\equiv$M′ bonds.[4,5] This led to the hypothesis that there was some special stability to the heteronuclear bonds, in particular the Mo$\equiv$W quadruple bonds. However, the first reported Mo$\equiv$W bonds in compounds with no bridging ligands were not specially short,[6] and therefore it became clear that, like other M–M multiple bonds, these are also subject to important influences by the appended ligands.[7] In order to increase our still rather sketchy knowledge of Mo$\equiv$W bonds, several new Mo$\equiv$WCl$_4$(L-L)$_2$ type complexes have been synthesized and characterized. The preparations, structures, and spectroscopic properties of two new classes of quadruply bonded heteronuclear compounds will be examined in this paper. Complexes **1–3** represent examples of a class of heteronuclear complexes containing only two bridging phosphine ligands, while complexes **4** and **5** represent the first heteronuclear dimers with chelate diphosphine ligands. In addition, the diamagnetic anisotropy of the Mo$\equiv$W bond has been estimated for complexes **1–4**.

Experimental Section

General Data. All manipulations were carried out under an atmosphere of argon unless otherwise specified. Standard Schlenk and vacuum line techniques were used. Commercial grade solvents, except alcohols and dichloromethane, were dried over and freshly distilled from potassium/sodium benzophenone ketyl prior to use. Alcohols and dichloromethane were dried over magnesium turnings and phosphorus pentoxide, respectively, and freshly distilled prior to use. Mo$\equiv$WCl$_4$(PMePh$_2$)$_4$ was prepared and purified by the literature method involving the reaction of Mo(η^6-C$_6$H$_5$PMePh)(PMePh$_2$)$_3$ with WCl$_4$(PPh$_3$)$_2$ in benzene.[8] Bidentate phosphines were purchased from Strem Chemicals and the solids dried in vacuo prior to use. The visible spectra were recorded on a Cary 17D spectrophotometer. The ^{31}P{^{1}H} NMR (81 MHz) and ^{1}H NMR (200 MHz) spectra were recorded on a Varian XL-200 spectrometer. The ^{31}P{^{1}H} NMR chemical shift values were referenced externally and are reported relative to 85% H$_3$PO$_4$.

Preparation of Mo$\equiv$WCl$_4$(μ-dppm)$_2$ (1). Mo$\equiv$WCl$_4$(PMePh$_2$)$_4$ (0.050 g, 0.041 mmol) and dppm (0.063 g, 0.164 mmol) were suspended in 20 mL of 1-propanol. This suspension was stirred and heated at reflux temperature for 4 h. Upon heating, the suspended solids dissolved, and after approximately 30 min a green precipitate began to form. Stirring and heating were continued for an additional 3^1/$_2$ h to ensure the completion of the reaction. The green precipitate was then filtered out, washed with hexanes, and dried in vacuo (0.029 g, 58%).

Preparation of β-Mo$\equiv$WCl$_4$(μ-dppe)$_2$ (2). Mo$\equiv$WCl$_4$(PMePh$_2$)$_4$ (0.050 g, 0.041 mmol) and dppe (0.063 g, 0.164 mmol) was suspended in 20 mL of 1-propanol. This suspension was stirred and heated at reflux temperature for 12 h. Upon heating the suspended solids dissolved, and after approximately 1 h a brown precipitate began to form. Stirring and

† Currently at Los Alamos National Laboratory, INC-14 MS345, Los Alamos, NM 87545.

(1) Morris, R. H. *Polyhedron* **1987**, *6*, 793.
(2) Cotton, F. A.; Favello, L. R.; Luck, R. L.; James, C. A. *Inorg. Chem.* **1990**, *29*, 4759.
(3) Cotton, F. A.; Luck, R. L.; James, C. A. *Inorg. Chem.* **1991**, *30*, 4370.
(4) McCarley, R. E.; Katovic, V. *J. Am. Chem. Soc.* **1978**, *100*, 5586.
(5) Cotton, F. A.; Hanson, B. E. *Inorg. Chem.* **1978**, *17*, 3237.
(6) McCarley, R. E.; Katovic, V. *J. Am. Chem. Soc.* **1975**, *97*, 5300.
(7) Cotton, F. A.; Walton, R. A. *Multiple Bonds Between Metal Atoms*, 2nd ed., Oxford University Press: Oxford, England, 1992.
(8) Morris, R. H.; Luck, R. H.; Sawyer, J. F. *Inorg. Chem.* **1987**, *26*, 2422.

0020-1669/92/1331-5298$03.00/0

Table I. Crystallographic Data and Data Collection Parameters for Mo≡WCl$_4$(μ-dppm)$_2$·2THF·C$_6$H$_6$ (**1**), β-Mo≡WCl$_4$(μ-dppe)$_2$ (**2**), and α-Mo≡WCl$_4$(dmpe)$_2$·4CH$_2$Cl$_2$ (**4**)

	1	**2**	**3**
chem formula	$WMoCl_4P_4OC_{66}H_{64}$	$WMoCl_4P_4C_{52}H_{48}$	$WMoCl_{12}P_4C_{16}H_{32}$
fw	1418.7	1218.5	1053.56
space group (no.)	$P2_1/c$ (14)	$P2_1/n$ (14)	$P2_1/c$ (14)
a, Å	21.562 (3)	23.099 (4)	10.422 (6)
b, Å	14.567 (4)	13.248 (1)	16.707 (6)
c, Å	22.063 (4)	16.765 (3)	11.406 (8)
α, deg	90	90	90
β, deg	118.82 (1)	107.45 (2)	111.87 (6)
γ, deg	90	90	90
V, Å^3	6071 (2)	4894 (2)	1843 (2)
Z	4	4	2
T, °C	23 ± 2	23 ± 2	−100 ± 2
λ, Å	0.710 73	1.541 84	0.710 73
ρ_{calcd}, g cm^{-3}	1.552	1.653	1.898
μ(Mo Kα or Cu Kα), cm^{-1}	24.582	100.772	45.611
transm coeff	0.9985–0.8986	1.000–0.7160	0.9965–0.254
$R(F_o)$,[a] $R_w(F_o)$[b]	0.0401, 0.0525	0.0539, 0.0622	0.1166, 0.1717

[a] $R = \sum||F_o| - |F_c||/\sum|F_o|$. [b] $R_w = [\sum w(|F_o| - |F_c|)^2/\sum w|F_o|^2]^{1/2}$; $w = 1/\sigma^2(|F_o|)$.

Table II. Positional and Thermal Parameters for Non-Hydrogen Atoms of Mo≡WCl$_4$(μ-dppm)$_2$ (**1**)

atom	x	y	z	B,[a] Å^2	atom	x	y	z	B,[a] Å^2
MW(1)[b]	0.25246 (2)	−0.08788 (3)	0.11924 (2)	2.81 (1)	C(125)	0.4297 (3)	−0.1434 (3)	0.0230 (3)	7.4 (4)
MW(2)	0.21210 (2)	0.01734 (3)	0.16364 (2)	2.73 (1)	C(126)	0.4013 (3)	−0.1093 (3)	0.0634 (3)	5.8 (3)
Cl(1)	0.1889 (1)	−0.0689 (1)	−0.00346 (9)	4.62 (6)	C(211)	0.1873 (2)	−0.3209 (4)	0.1496 (3)	3.9 (2)
Cl(2)	0.35346 (9)	−0.1623 (1)	0.2084 (1)	4.62 (6)	C(212)	0.1429 (2)	−0.3694 (4)	0.1678 (3)	5.9 (4)
Cl(3)	0.2882 (1)	0.0287 (1)	0.28546 (9)	4.56 (6)	C(213)	0.1660 (2)	−0.4514 (4)	0.2046 (3)	8.7 (6)
Cl(4)	0.09865 (9)	0.0575 (1)	0.0708 (1)	4.45 (6)	C(214)	0.2335 (2)	−0.4850 (4)	0.2233 (3)	7.3 (4)
P(1)	0.33874 (9)	0.0177 (1)	0.10807 (9)	3.41 (5)	C(215)	0.2778 (2)	−0.4364 (4)	0.2051 (3)	6.8 (4)
P(2)	0.15867 (9)	−0.2160 (1)	0.09900 (9)	3.36 (6)	C(216)	0.2547 (2)	−0.3544 (4)	0.1683 (3)	5.4 (3)
P(3)	0.14031 (9)	−0.0917 (1)	0.19367 (9)	3.13 (5)	C(221)	0.1044 (3)	−0.2591 (3)	0.0112 (3)	3.8 (2)
P(4)	0.2556 (1)	0.1642 (1)	0.12671 (9)	3.44 (6)	C(222)	0.1180 (3)	−0.3458 (3)	−0.0065 (3)	6.3 (3)
C(1)	0.2437 (7)	0.3085 (9)	0.3974 (6)	8.9 (5)	C(223)	0.0767 (3)	−0.3793 (3)	−0.0735 (3)	7.4 (4)
C(2)	0.2208 (9)	0.229 (1)	0.3626 (8)	12.6 (7)	C(224)	0.0218 (3)	−0.3260 (3)	−0.1228 (3)	6.8 (4)
C(3)	0.1595 (9)	0.250 (1)	0.2886 (8)	13.5 (7)	C(225)	0.0082 (3)	−0.2393 (3)	−0.1051 (3)	6.0 (3)
C(4)	0.141 (1)	0.340 (1)	0.296 (1)	17.4 (8)	C(226)	0.0495 (3)	−0.2058 (3)	−0.0382 (3)	5.1 (3)
C(5)	0.201 (1)	0.377 (1)	0.3623 (8)	14.6 (8)	C(311)	0.1783 (2)	−0.1711 (3)	0.2658 (2)	3.3 (2)
C(14)	0.2918 (4)	0.1245 (5)	0.0710 (3)	3.7 (2)	C(312)	0.2486 (2)	−0.1984 (3)	0.2918 (2)	4.4 (2)
C(23)	0.0931 (3)	−0.1654 (5)	0.1186 (4)	3.6 (2)	C(313)	0.2777 (2)	−0.2636 (3)	0.3446 (2)	5.4 (3)
C(31)	0.507 (2)	0.332 (2)	0.100 (1)	14 (1)	C(314)	0.2366 (2)	−0.3013 (3)	0.3714 (2)	5.5 (3)
C(32)	0.5397 (9)	0.382 (1)	0.072 (1)	14.0 (9)	C(315)	0.1663 (2)	−0.2740 (3)	0.3455 (2)	5.0 (3)
C(33)	0.511 (1)	0.381 (2)	−0.001 (1)	15 (1)	C(316)	0.1372 (2)	−0.2089 (3)	0.2926 (2)	4.5 (3)
C(34)	0.446 (1)	0.351 (2)	−0.0361 (9)	12.6 (9)	C(321)	0.0747 (2)	−0.0320 (3)	0.2082 (2)	3.7 (2)
C(35)	0.421 (1)	0.295 (1)	−0.006 (1)	12.6 (9)	C(322)	0.0987 (2)	0.0067 (3)	0.2735 (2)	4.4 (2)
C(36)	0.445 (1)	0.285 (1)	0.057 (1)	13.5 (9)	C(323)	0.0522 (2)	0.0561 (3)	0.2884 (2)	5.4 (3)
C(41)	0.324 (1)	0.541 (3)	0.058 (1)	28 (2)	C(324)	−0.0183 (2)	0.0667 (3)	0.2379 (2)	6.2 (4)
C(42)	0.316 (1)	0.606 (2)	0.012 (1)	19 (1)	C(325)	−0.0424 (2)	0.0280 (3)	0.1725 (2)	5.9 (3)
C(43)	0.268 (1)	0.558 (1)	−0.0541 (7)	14.5 (9)	C(326)	0.0041 (2)	−0.0214 (3)	0.1576 (2)	4.4 (2)
C(44)	0.241 (1)	0.481 (1)	−0.040 (1)	15 (1)	C(411)	0.1857 (3)	0.2442 (4)	0.0714 (3)	4.2 (2)
C(45)	0.288 (2)	0.468 (2)	0.033 (2)	24 (2)	C(412)	0.1436 (3)	0.2258 (4)	0.0010 (3)	5.9 (3)
C(111)	0.4217 (2)	0.0544 (4)	0.1811 (3)	3.5 (2)	C(413)	0.0891 (3)	0.2858 (4)	−0.0405 (3)	7.6 (4)
C(112)	0.4310 (2)	0.0497 (4)	0.2481 (3)	4.9 (3)	C(414)	0.0766 (3)	0.3641 (4)	−0.0117 (3)	7.8 (4)
C(113)	0.4911 (2)	0.0879 (4)	0.3031 (3)	6.3 (3)	C(415)	0.1186 (3)	0.3825 (4)	0.0587 (3)	9.8 (5)
C(114)	0.5421 (2)	0.1307 (4)	0.2911 (3)	6.3 (3)	C(416)	0.1732 (3)	0.3226 (4)	0.1002 (3)	7.0 (4)
C(115)	0.5328 (2)	0.1354 (4)	0.2241 (3)	6.0 (3)	C(421)	0.3219 (3)	0.2406 (4)	0.1901 (3)	4.0 (2)
C(116)	0.4726 (2)	0.0973 (4)	0.1691 (3)	5.3 (3)	C(422)	0.3278 (3)	0.2459 (4)	0.2558 (3)	6.9 (4)
C(121)	0.3674 (3)	−0.0242 (3)	0.0480 (3)	4.0 (2)	C(423)	0.3754 (3)	0.3073 (4)	0.3045 (3)	8.4 (4)
C(122)	0.3619 (3)	0.0268 (3)	−0.0080 (3)	6.1 (4)	C(424)	0.4172 (3)	0.3635 (4)	0.2875 (3)	7.7 (4)
C(123)	0.3903 (3)	−0.0074 (3)	−0.0484 (3)	7.4 (4)	C(425)	0.4113 (3)	0.3583 (4)	0.2218 (3)	8.0 (5)
C(124)	0.4242 (3)	−0.0924 (3)	−0.0330 (3)	8.0 (4)	C(426)	0.3637 (3)	0.2968 (4)	0.1731 (3)	6.7 (4)

[a] B values for anisotropically refined atoms are given in the form of the equivalent isotropic displacement parameter defined as $^1/_3[a^2a^{*2}B_{11} + b^2b^{*2}B_{22} + c^2c^{*2}B_{33} + 2ab(\cos\gamma)a^*b^*B_{12} + 2ac(\cos\beta)a^*c^*B_{13} + 2bc(\cos\alpha)b^*c^*B_{23}]$. [b] Hybrid metal atom composed of 58.1 (3)% Mo and 41.9 (3)% W.

heating were continued for an additional 11 h to ensure the completion of the reaction. The brown precipitate was then filtered out, washed with hexanes, and dried in vacuo (0.024 g, 48%).

Preparation of α-Mo≡WCl$_4$(dppe)$_2$ (5). Mo≡WCl$_4$(PMePh$_2$)$_4$ (0.050 g, 0.041 mmol) and dppe (0.063 g, 0.164 mmol) were suspended in 20 mL of methanol. This suspension was stirred at ambient temperature for 48 h. The color of the suspension gradually changed from green to blue during the course of the reaction. The blue precipitate was then filtered out, washed with benzene and hexanes, and dried in vacuo (0.34 g, 68%).

Isomerization Reaction. α-Mo≡WCl$_4$(dppe)$_2$ (**5**) was converted to β-Mo≡WCl$_4$(μ-dppe)$_2$ (**2**) after 36 h reflux in 1-propanol. The isolated product was shown to be β-Mo≡WCl$_4$(μ-dppe)$_2$ by its visible spectrum.

Preparation of Mo≡WCl$_4$(μ-dmpm)$_2$ (3). Method 1. Mo≡WCl$_4$(PMePh$_2$)$_4$ (0.050 g, 0.041 mmol) and dmpm (0.014 g, 0.1025 mmol) were suspended in a mixture of 10 mL of hexanes and 5 mL of benzene. This suspension was stirred at ambient temperature for 1 h, and then the solvents were removed in vacuo leaving an oily green residue. This residue was then extracted with 3 × 5 mL portions of toluene and immediately

cooled to −78 °C. This solution was used for spectroscopic measurements, but no yields were measured for this preparative route.

Method 2. $Mo{\equiv}WCl_4(PMePh_2)_4$ (0.050 g, 0.041 mmol) was dissolved in 10 mL of benzene in a Schlenk tube. A mixture of benzene and hexanes (1:2) was then layered above this solution. Finally, 0.045 g (0.348 mmol) of dmpm dissolved in 20 mL of hexanes was layered over the benzene/hexanes solvent mixture. This layered mixture was left undisturbed for 1 week producing 0.013 g (46%) of crystalline $Mo{\equiv}WCl_4(\mu\text{-dmpm})_2$.

Preparation of α-$Mo{\equiv}WCl_4(dmpe)_2$ (4). $Mo{\equiv}WCl_4(PMePh_2)_4$ (0.050 g, 0.041 mmol) and dmpe (0.049 g, 0.328 mmol) were suspended in a mixture of 10 mL of hexanes and 5 mL of benzene. This suspension was stirred at room temperature for 12 h resulting in a blue precipitate. The blue precipitate was filtered out, washed with hexanes, and dried in vacuo (0.019 g, 64%).

X-ray Crystallography

Single crystals of **1** and **2** were obtained by layering dilute THF solutions of the compounds with a mixture of benzene and methanol (1:2) in long glass tubes sealed under an argon atmosphere. Single crystals of **3** were obtained by method 2 as described in the Experimental Section, and crystals of complex **4** were obtained by cooling a CH_2Cl_2 solution to −78 °C and maintaining this temperature for several days. The crystals of **1** and **2** were coated with a thin layer of epoxy and mounted on the tip of a glass fiber. The crystal of **4** was mounted at −80 °C on a quartz fiber in silicone grease saturated with CH_2Cl_2.

Single-crystal diffraction experiments were conducted on either Enraf-Nonius CAD4 or Rigaku AFC5 automated diffractometers using Mo Kα and Cu Kα radiation, respectively. Routine unit cell identification and intensity data collection procedures were followed utilizing the options specified in Table I and the general procedures previously described.[9] Lattice dimensions and Laue symmetry were verified using axial photographs. Three standard reflections were measured every 1 h during data collections to monitor any gain or loss in intensity, and a correction was made when ΔI was greater than 5%. Corrections for Lorentz, polarization, and absorption effects were applied to all data sets. The latter correction was based on azimuthal scans of several reflections with diffractometer angle χ near 90°.[10]

General Structure Solution and Refinement. The following general procedures were employed for the solution and refinement of all compounds unless otherwise noted.

The heavy-atom positions were obtained from three-dimensional Patterson functions. Hybrid atoms (MW) composed of 50% Mo and 50% W were placed at the metal atom positions in the initial stages of the refinement. The positions for the remainder of the non-hydrogen atoms were found using a series of full matrix refinements followed by difference Fourier syntheses. These positions were initially refined with isotropic thermal parameters and then with anisotropic thermal parameters to convergence. The hydrogen atoms, where included, were placed and fixed at calculated positions and their isotropic thermal parameters constrained to one variable, and the entire model was refined to convergence. Final refinements employed the SHELX-76 package of programs with variations in occupancy factors used to determine the composition of the metal atoms sites. Important details pertinent to individual compounds are presented in Table I and in the following paragraphs.

Compound 1. The difference Fourier map showed several peaks that could be ascribed to solvent molecules, namely two THF molecules and one benzene molecule. All atoms representing these solvent molecules were allowed to refine freely first with isotropic and then anisotropic thermal parameters to convergence. The composition of the hybrid metal atom was 58.1 (3)% Mo and 41.9 (3)% W at convergence. The final refinement factors after convergence are listed in Table I. Table II contains positional and thermal parameters for non-hydrogen atoms. Selected bond lengths and angles are listed in Table III, and an ORTEP diagram of the molecule is given in Figure 1. Tables of anisotropic thermal parameters, complete bond lengths and angles, and hydrogen atom positional parameters and a complete ORTEP diagram are available as supplementary material.

Compound 2. In the case of **2** a sudden rapid loss of intensity, as the result of a sudden increase in room temperature, required that nonstandard techniques be employed to correct for the nonlinear decay. The original data set was separated into two sets, one before the decay and another after the decay. The data sets were then merged utilizing the SHELX-76 package of programs. The agreement factor for the merge was 0.015. Standard data reduction procedures were then employed prior to structure solution and refinement.

The difference Fourier map revealed the presence of two additional metal atoms. The magnitude of these peaks showed that this M–M′ unit, which formed a perpendicular bisector of the MW(1)–MW(2) bond, was present in relatively low abundance. Hybrid metal atoms were placed in the positions indicated by the difference Fourier map. The occupancies for both the major and minor orientations were fixed at 0.92 and 0.08, respectively. This model was then refined, first with isotropic and then anisotropic thermal parameters, to convergence.

Variations in occupancy factors were first used to determine the occupancies of the major and minor hybrid metal atom sites by constraining them so that the average occupancy of the principal sites plus the average occupancy of the minor sites was equal to one. Variations in occupancy factors were again used to determine the composition of the hybrid metal atom at all four sites. The composition of the hybrid atom was determined by constraining it such that % Mo + % W = 100 and refining these occupancies.

Final values for the occupancy factors for the major and minor orientations and hybrid metal atom composition were obtained by alternating the procedures described above until the calculations converged. The final values for the occupancy factors for the major and minor metal atom sites were 93.1 (6)% and 6.9 (6) %, while the composition of the hybrid metal atom was 62.1 (6)% Mo and 37.9 (6)% W.

The final refinement factors after convergence are listed in Table I. Table IV contains positional and thermal parameters for non-hydrogen atoms. Selected bond lengths and angles are listed in Table V. ORTEP diagrams of the molecule are given in Figures 2 and 3, while tables of anisotropic thermal parameters, complete bond lengths and angles, and hydrogen atom positional parameters and a complete ORTEP drawing are available as supplementary material.

Table III. Selected Bond Lengths (Å) and Angles (deg) for $Mo{\equiv}WCl_4(\mu\text{-dppm})_2$ (**1**)[a]

Distances			
MW(1)[b]–MW(2)	2.2110 (7)	P(1)–C(121)	1.817 (8)
MW(1)–Cl(1)	2.389 (2)	P(2)–C(23)	1.822 (9)
MW(1)–Cl(2)	2.378 (2)	P(2)–C(211)	1.816 (6)
MW(1)–P(1)	2.516 (2)	P(2)–C(221)	1.825 (5)
MW(1)–P(2)	2.627 (2)	P(3)–C(23)	1.818 (7)
MW(2)–Cl(3)	2.386 (2)	P(3)–C(311)	1.813 (5)
MW(2)–Cl(4)	2.386 (2)	P(3)–C(321)	1.816 (6)
MW(2)–P(3)	2.519 (2)	P(4)–C(14)	1.840 (9)
MW(2)–P(4)	2.618 (2)	P(4)–C(411)	1.829 (5)
P(1)–C(14)	1.821 (7)	P(4)–C(421)	1.820 (5)
P(1)–C(111)	1.818 (4)		
Angles			
MW(2)–MW(1)–Cl(1)	106.77 (6)	MW(1)–P(1)–C(121)	113.2 (2)
MW(2)–MW(1)–Cl(2)	110.42 (6)	C(14)–P(1)–C(111)	104.0 (3)
MW(2)–MW(1)–P(1)	95.01 (5)	C(14)–P(1)–C(121)	105.7 (3)
MW(2)–MW(1)–P(2)	97.63 (5)	C(111)–P(1)–C(121)	102.1 (3)
Cl(1)–MW(1)–Cl(2)	141.83 (8)	MW(1)–P(2)–C(23)	107.1 (2)
Cl(1)–MW(1)–P(1)	82.29 (7)	MW(1)–P(2)–C(211)	119.2 (2)
Cl(1)–MW(1)–P(2)	85.14 (7)	MW(1)–P(2)–C(221)	118.1 (2)
Cl(2)–MW(1)–P(1)	86.21 (6)	C(23)–P(2)–C(211)	105.5 (3)
Cl(2)–MW(1)–P(2)	98.02 (6)	C(23)–P(2)–C(221)	102.6 (3)
P(1)–MW(1)–P(2)	164.29 (7)	C(211)–P(2)–C(221)	102.6 (2)
MW(1)–MW(2)–Cl(3)	110.10 (6)	MW(2)–P(3)–C(23)	106.1 (3)
MW(1)–MW(2)–Cl(4)	104.43 (6)	MW(2)–P(3)–C(311)	124.0 (2)
MW(1)–MW(2)–P(3)	95.89 (5)	MW(2)–P(3)–C(321)	112.0 (2)
MW(1)–MW(2)–P(4)	98.75 (6)	C(23)–P(3)–C(311)	103.9 (3)
Cl(3)–MW(2)–Cl(4)	144.48 (8)	C(23)–P(3)–C(321)	107.6 (3)
Cl(3)–MW(2)–P(3)	85.61 (7)	C(311)–P(3)–C(321)	102.2 (3)
Cl(3)–MW(2)–P(4)	97.98 (6)	MW(2)–P(4)–C(14)	106.4 (2)
Cl(4)–MW(2)–P(3)	82.82 (6)	MW(2)–P(4)–C(411)	115.2 (2)
Cl(4)–MW(2)–P(4)	84.54 (6)	MW(2)–P(4)–C(421)	121.9 (2)
P(3)–MW(2)–P(4)	162.64 (7)	C(14)–P(4)–C(411)	103.5 (3)
MW(1)–P(1)–C(14)	106.8 (3)	C(14)–P(4)–C(421)	106.0 (3)
MW(1)–P(1)–C(111)	123.5 (2)	C(411)–P(4)–C(421)	102.3 (3)

[a] Numbers in parentheses are estimated standard deviations in the least significant digit. [b] Hybrid metal atom composed of 58.1 (3)% Mo and 41.9 (3)% W.

(9) Bino, A.; Cotton, F. A.; Fanwick, P. E. *Inorg. Chem.* **1979**, *18*, 3558.
(10) North, A. C. T.; Phillips, D. A.; Matthews, F. S. *Acta Crystallogr., Sect. A: Cryst. Phys., Diffr., Theor. Gen. Crystallogr.* **1968**, *24A*, 351.

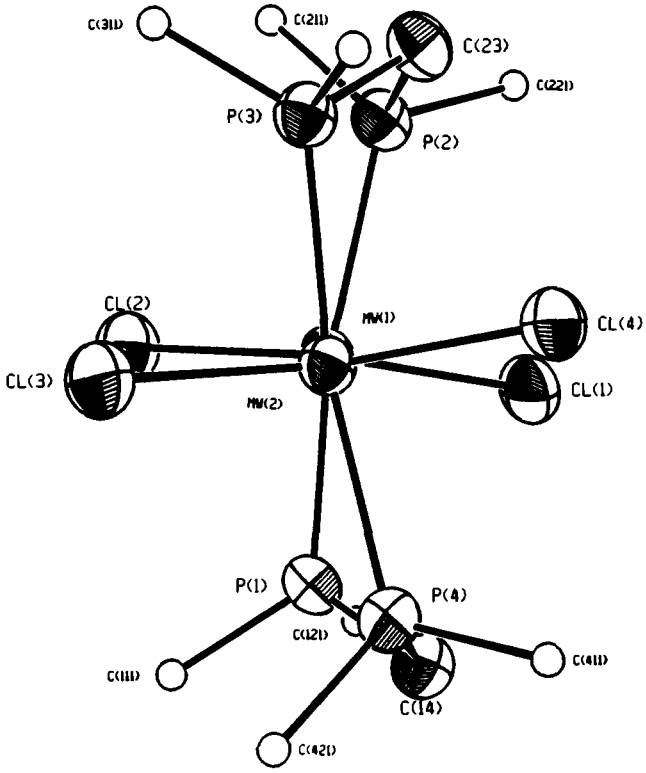

Figure 1. ORTEP drawing of $Mo_4^{4+}WCl_4(\mu\text{-dppm})_2$ showing the torsional angle (phenyl rings of dppm omitted). Thermal ellipsoids, except carbons, are drawn at 50% probability. The carbon atoms are shown as arbitrarily sized uniform circles.

Compound 3. The crystallographic details for this compound will be reported later where comparisons with other $M_2X_4(dmpm)_2$ compounds will be made.

Compound 4. The difference Fourier map showed several peaks that could be ascribed to solvent molecules. These peaks were modeled as two CH_2Cl_2 solvent molecules, and the entire model was allowed to refine freely with isotropic thermal parameters to convergence. Because the residuals remained high at this point in the refinement, a calculated absorption correction utilizing the DIFABS[11] program was applied to the data set. After the application of this correction, the model was allowed to refine freely first with isotropic and then finally anisotropic thermal parameters to convergence. Both the initial refinement of the hybrid metal atom composition and the $^{31}P\{^1H\}$ NMR failed to indicate the presence of $\alpha\text{-}Mo_4^{4+}MoCl_4(dmpe)_2$. Therefore, the hybrid metal atom composition was fixed at 50.0% Mo and 50.0% W in the final refinement. The final refinement factors after convergence are listed in Table I. Table VI contains positional and thermal parameters. Complete bond lengths and angles are listed in Tables VII and VIII. An ORTEP drawing of the molecule is given in Figure 4, while tables of anisotropic thermal parameters are available as supplementary material.

Results and Discussion

Synthesis. Preliminary investigations into the solution chemistry of $Mo_4^{4+}WCl_4(PMePh_2)_4$ indicate that similarities exist between the molybdenum–tungsten system and both the dimolybdenum and ditungsten systems. Relative to dimolybdenum systems, an increased sensitivity to oxidation is the most notable similarity between the MoW and WW systems. The sensitivity of tungsten dimers to oxidation has been well documented in the literature,[12-15] and many of the analogous dinuclear Mo–W compounds exhibit almost identical behavior.[3,16,17] Parallels between the heteronuclear systems and the dimolybdenum system

Table IV. Positional and Thermal Parameters for Non-Hydrogen Atoms of $\beta\text{-}Mo_4^{4+}WCl_4(\mu\text{-dppe})_2$ (**2**)

atom	*x*	*y*	*z*	*B*,[a] Å^2
MW(1)[b]	0.25051 (4)	0.20023 (7)	0.03490 (6)	3.21 (3)
MW(2)	0.31117 (4)	0.29971 (7)	−0.01326 (6)	3.54 (3)
MW(3)	0.2427 (6)	0.285 (1)	−0.028 (1)	4.9 (5)
MW(4)	0.3159 (7)	0.227 (1)	0.065 (1)	4.1 (4)
Cl(1)	0.2869 (2)	0.1664 (3)	0.1822 (3)	5.7 (1)
Cl(2)	0.1629 (2)	0.1550 (3)	−0.0745 (3)	5.8 (1)
Cl(3)	0.4068 (2)	0.2232 (3)	0.0019 (3)	5.3 (1)
Cl(4)	0.2648 (2)	0.4588 (3)	−0.0635 (3)	5.1 (1)
P(1)	0.1959 (2)	0.3396 (3)	0.0904 (3)	4.7 (1)
P(2)	0.2938 (2)	0.0338 (3)	0.0017 (3)	5.1 (1)
P(3)	0.2853 (2)	0.2256 (3)	−0.1613 (3)	5.2 (1)
P(4)	0.3547 (2)	0.4003 (3)	0.1200 (3)	4.6 (1)
C(14)	0.2500 (6)	0.414 (1)	0.172 (1)	5.5 (5)
C(23)	0.2793 (7)	0.021 (1)	−0.111 (1)	6.0 (6)
C(32)	0.3090 (8)	0.096 (1)	−0.159 (1)	5.9 (5)
C(41)	0.2975 (7)	0.474 (1)	0.150 (1)	5.2 (5)
C(111)	0.1464 (7)	0.282 (1)	0.1434 (7)	5.6 (6)
C(112)	0.0982 (7)	0.226 (1)	0.0931 (7)	7.7 (7)
C(113)	0.0562 (7)	0.182 (1)	0.1276 (7)	8.5 (8)
C(114)	0.0624 (7)	0.195 (1)	0.2123 (7)	8.7 (9)
C(115)	0.1106 (7)	0.251 (1)	0.2626 (7)	8.4 (8)
C(116)	0.1526 (7)	0.295 (1)	0.2282 (7)	6.7 (6)
C(122)	0.1169 (6)	0.5062 (8)	0.067 (1)	7.9 (8)
C(123)	0.0737 (6)	0.5725 (8)	0.018 (1)	8.7 (9)
C(124)	0.0561 (6)	0.5649 (8)	−0.069 (1)	8.2 (9)
C(125)	0.0817 (6)	0.4909 (8)	−0.107 (1)	7.6 (7)
C(126)	0.1248 (6)	0.4245 (8)	−0.058 (1)	6.3 (6)
C(121)	0.1424 (6)	0.4321 (8)	0.029 (1)	4.7 (5)
C(211)	0.3711 (7)	−0.0051 (9)	0.0527 (7)	4.6 (5)
C(212)	0.4083 (7)	−0.0426 (9)	0.0075 (7)	7.2 (7)
C(213)	0.4665 (7)	−0.0774 (9)	0.0496 (7)	8.1 (9)
C(214)	0.4874 (7)	−0.0748 (9)	0.1367 (7)	9.3 (9)
C(215)	0.4503 (7)	−0.0373 (9)	0.1818 (7)	9.6 (8)
C(216)	0.3921 (7)	−0.0025 (9)	0.1398 (7)	6.2 (6)
C(221)	0.2537 (6)	−0.0744 (9)	0.0238 (8)	6.3 (6)
C(222)	0.2120 (6)	−0.0637 (9)	0.0686 (8)	7.9 (8)
C(223)	0.1834 (6)	−0.1486 (9)	0.0884 (8)	12 (1)
C(224)	0.1964 (6)	−0.2442 (9)	0.0635 (8)	13 (1)
C(225)	0.2381 (6)	−0.2549 (9)	0.0187 (8)	14 (1)
C(226)	0.2668 (6)	−0.1700 (9)	−0.0011 (8)	9.6 (8)
C(311)	0.2114 (6)	0.2333 (8)	−0.2370 (7)	5.5 (6)
C(312)	0.1755 (6)	0.3175 (8)	−0.2354 (7)	5.8 (6)
C(313)	0.1173 (6)	0.3248 (8)	−0.2916 (7)	7.4 (7)
C(314)	0.0950 (6)	0.2479 (8)	−0.3496 (7)	9.5 (8)
C(315)	0.1309 (6)	0.1637 (8)	−0.3512 (7)	11.7 (9)
C(316)	0.1891 (6)	0.1564 (8)	−0.2949 (7)	7.4 (7)
C(321)	0.3311 (6)	0.280 (1)	−0.2222 (8)	5.2 (5)
C(322)	0.3457 (6)	0.383 (1)	−0.2107 (8)	8.6 (8)
C(323)	0.3760 (6)	0.430 (1)	−0.2609 (8)	9.7 (9)
C(324)	0.3916 (6)	0.376 (1)	−0.3225 (8)	8.5 (8)
C(325)	0.3770 (6)	0.273 (1)	−0.3339 (8)	10 (1)
C(326)	0.3467 (6)	0.226 (1)	−0.2838 (8)	11 (1)
C(411)	0.4022 (5)	0.499 (1)	0.0991 (8)	5.0 (5)
C(412)	0.3821 (5)	0.598 (1)	0.0767 (8)	6.8 (7)
C(413)	0.4218 (5)	0.670 (1)	0.0619 (8)	7.7 (8)
C(414)	0.4817 (5)	0.643 (1)	0.0695 (8)	7.8 (8)
C(415)	0.5019 (5)	0.545 (1)	0.0919 (8)	8.9 (9)
C(416)	0.4621 (5)	0.473 (1)	0.1067 (8)	7.7 (7)
C(421)	0.4035 (7)	0.3516 (9)	0.217 (1)	6.0 (6)
C(422)	0.4255 (7)	0.4129 (9)	0.288 (1)	10.5 (9)
C(423)	0.4700 (7)	0.3766 (9)	0.358 (1)	13 (1)
C(424)	0.4925 (7)	0.2789 (9)	0.358 (1)	9.7 (9)
C(425)	0.4705 (7)	0.2175 (9)	0.287 (1)	9.4 (8)
C(426)	0.4260 (7)	0.2539 (9)	0.217 (1)	7.1 (7)

[a] Anisotropically refined atoms are given in the form of the equivalent isotropic displacement parameter defined as $^1/_3[a^2a^{*2}B_{11} + b^2b^{*2}B_{22} + c^2c^{*2}B_{33} + 2ab(\cos\gamma)a^*b^*B_{12} + 2ac(\cos\beta)a^*c^*B_{13} + 2bc(\cos\alpha)b^*c^*B_{23}]$. [b] Hybrid metal atom composed of 62.1 (6)% Mo and 37.9 (6)% W.

(11) North, A. C. T.; Phillips, D. A.; Matthews, F. S. *Acta Crystallogr.* **1983**, *A39*, 159.
(12) Sattelberger, A. P.; McLaughlin, K. W.; Huffman, J. C. *J. Am. Chem. Soc.* **1981**, *103*, 2280.
(13) Cotton, F. A.; Mott, G. N. *J. Am. Chem. Soc.* **1982**, *104*, 5978.
(14) Fanwick, P. E.; Harwood, W. S.; Walton, R. A. *Inorg. Chem.* **1987**, *26*, 242.
(15) Canich, J. M.; Cotton, F. A.; Daniels, L. M.; Lewis, D. B. *Inorg. Chem.* **1987**, *26*, 4046.
(16) McCarley, R. E.; Katovic, V. *Inorg. Chem.* **1978**, *17*, 1268.

Table V. Selected Bond Lengths (Å) and Angles (deg) for β-Mo≡^{4}WCl$_4$(μ-dppe)$_2$ (**2**)[a]

Distances			
MW(1)[b]–MW(2)	2.243 (1)	MW(4)–Cl(3)	2.61 (2)
MW(1)–Cl(1)	2.401 (4)	MW(4)–P(2)	2.76 (1)
MW(1)–Cl(2)	2.365 (3)	MW(4)–P(4)	2.54 (1)
MW(1)–P(1)	2.563 (5)	P(1)–C(14)	1.84 (1)
MW(1)–P(2)	2.550 (4)	P(1)–C(111)	1.81 (2)
MW(2)–Cl(3)	2.373 (4)	P(1)–C(121)	1.83 (1)
MW(2)–Cl(4)	2.399 (4)	P(2)–C(23)	1.83 (2)
MW(2)–P(3)	2.567 (5)	P(2)–C(211)	1.81 (1)
MW(2)–P(4)	2.536 (4)	P(2)–C(221)	1.81 (1)
MW(3)–MW(4)	2.07 (2)	P(3)–C(32)	1.80 (1)
MW(3)–Cl(2)	2.47 (2)	P(3)–C(311)	1.80 (1)
MW(3)–Cl(4)	2.47 (2)	P(3)–C(321)	1.83 (2)
MW(3)–P(1)	2.63 (2)	P(4)–C(41)	1.83 (2)
MW(3)–P(3)	2.81 (2)	P(4)–C(411)	1.81 (1)
MW(4)–Cl(1)	2.40 (2)	P(4)–C(421)	1.80 (2)
Angles			
MW(2)–MW(1)–Cl(1)	114.6 (1)	Cl(2)–MW(3)–P(1)	89.6 (6)
MW(2)–MW(1)–Cl(2)	110.6 (1)	Cl(2)–MW(3)–P(3)	87.7 (5)
MW(2)–MW(1)–P(1)	97.8 (1)	Cl(4)–MW(3)–P(1)	95.0 (6)
MW(2)–MW(1)–P(2)	95.8 (1)	Cl(4)–MW(3)–P(3)	85.5 (5)
Cl(1)–MW(1)–Cl(2)	134.8 (2)	P(1)–MW(3)–P(3)	176.4 (6)
Cl(1)–MW(1)–P(1)	79.6 (1)	MW(3)–MW(4)–Cl(1)	111.9 (9)
Cl(1)–MW(1)–P(2)	91.4 (1)	MW(3)–MW(4)–Cl(3)	106.3 (8)
Cl(2)–MW(1)–P(1)	93.7 (1)	MW(3)–MW(4)–P(2)	92.4 (6)
Cl(2)–MW(1)–P(2)	85.0 (1)	MW(3)–MW(4)–P(4)	93.4 (6)
P(1)–MW(1)–P(2)	165.9 (2)	Cl(1)–MW(4)–Cl(3)	141.1 (6)
MW(1)–MW(2)–Cl(3)	111.9 (1)	Cl(1)–MW(4)–P(2)	86.4 (4)
MW(1)–MW(2)–Cl(4)	112.4 (1)	Cl(1)–MW(4)–P(4)	99.0 (6)
MW(1)–MW(2)–P(3)	97.7 (1)	Cl(3)–MW(4)–P(2)	84.6 (5)
MW(1)–MW(2)–P(4)	96.7 (1)	Cl(3)–MW(4)–P(4)	85.8 (5)
Cl(3)–MW(2)–Cl(4)	135.7 (1)	P(2)–MW(4)–P(4)	169.9 (7)
Cl(3)–MW(2)–P(3)	83.1 (1)	C(14)–P(1)–C(111)	104.2 (7)
Cl(3)–MW(2)–P(4)	91.1 (1)	C(14)–P(1)–C(121)	104.7 (6)
Cl(4)–MW(2)–P(3)	92.7 (1)	C(111)–P(1)–C(121)	97.9 (7)
Cl(4)–MW(2)–P(4)	82.2 (1)	C(23)–P(2)–C(211)	108.1 (7)
P(3)–MW(2)–P(4)	165.6 (2)	C(23)–P(2)–C(221)	100.9 (7)
MW(4)–MW(3)–Cl(2)	110.1 (8)	C(211)–P(2)–C(221)	99.8 (6)
MW(4)–MW(3)–Cl(4)	110.1 (7)	C(32)–P(3)–C(311)	106.7 (6)
MW(4)–MW(3)–P(1)	88.0 (8)	C(32)–P(3)–C(321)	99.7 (8)
MW(4)–MW(3)–P(3)	95.1 (8)	C(311)–P(3)–C(321)	99.7 (6)
Cl(2)–MW(3)–Cl(4)	139.7 (6)	C(41)–P(4)–C(411)	101.5 (7)
C(41)–P(4)–C(421)	104.4 (8)	C(411)–P(4)–C(421)	100.6 (6)

[a] Numbers in parentheses are estimated standard deviations in the least significant digit. [b] Hybrid metal atom composed of 62.1 (6)% Mo and 37.9 (6)% W.

are observed in the reduced reactivity of these compounds toward alcohols.[18,19] The molybdenum–tungsten and dimolybdenum species are stable in alcohols, but there have been no ditungsten preparations in alcohols reported. In addition, attempts in this laboratory to synthesize ditungsten complexes in alcohols have been unsuccessful.

The reactions involving Mo≡^{4}WCl$_4$(PMePh$_2$)$_4$ and dppm or dppe to form quadruply bonded complexes in alcohols are similar to those of their molybdenum counterparts.[18] Mo≡^{4}WCl$_4$(μ-dppm)$_2$ (**1**), β-Mo≡^{4}WCl$_4$(μ-dppe)$_2$ (**2**), and α-Mo≡^{4}WCl$_4$(dppe)$_2$ (**5**) are formed straightforwardly from the reaction of Mo≡^{4}WCl$_4$(PMePh$_2$)$_4$ with the appropriate bidentate phosphine ligand in 1-propanol or methanol. However, if the reactions are performed in aromatic or halocarbon solvents, edge-sharing bioctahedral rather than quadruply bonded products are formed. The reactions of Mo≡^{4}WCl$_4$(PMePh$_2$)$_4$ with either dppm or dppe, in hydrocarbon solvents, form MoWCl$_4$(μ-Cl)(μ-H)(μ-dppm)$_2$[3] or MoWCl$_6$(dppe)$_2$.[17] Reactions involving dmpe or dmpm in purely aromatic solvents also fail to yield quadruply bonded products but instead produce MoWCl$_6$(dmpe)$_2$[17] and an

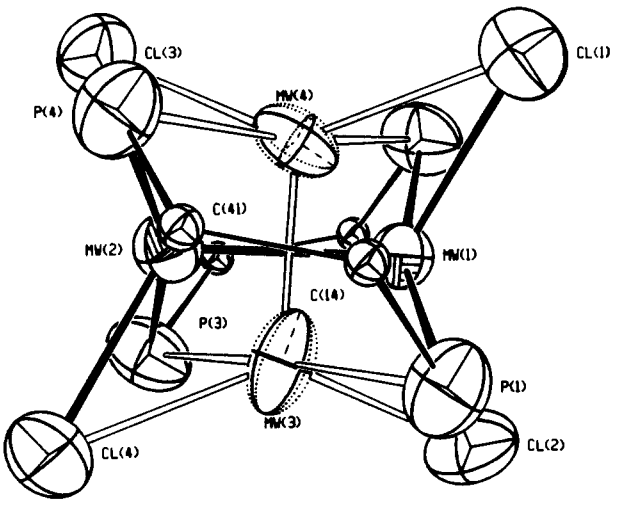

Figure 2. ORTEP drawing of β-Mo≡^{4}WCl$_4$(μ-dppe)$_2$ with both the major (—) and minor (- - -) orientations (phenyl rings of dppe omitted). Thermal ellipsoids, except carbons, are drawn at 50% probability. The carbon atoms are shown as arbitrarily sized uniform spheres.

uncharacterized red paramagnetic material, respectively. One might presume this product to be the MoW analog of the red, paramagnetic product obtained from the reaction of W$_2$Cl$_4$(PBu$_3$)$_4$ and dmpm, [Cl$_2$W(μ-dmpm)$_2$(μ-Cl)(μ-PMe$_2$)WCl(η^2-CH$_2$PMe$_2$]Cl, but there is no definitive proof.[20,21]

In order to promote the formation of quadruply bonded over edge-sharing products it is necessary to use a solvent mixture of benzene and *n*-hexanes (1:2). When Mo≡^{4}WCl$_4$(PMePh$_2$)$_4$ and dmpe or dmpm are allowed to react in this solvent mixture, the major products are α-Mo≡^{4}WCl$_4$(dmpe)$_2$ and Mo≡^{4}WCl$_4$(μ-dmpm)$_2$, respectively. The synthetic routes leading to the formation of quadruply bonded products all require a solvent or solvent mixture in which the products are insoluble. This insolubility causes the quadruply bonded products to precipitate from solution and prevents oxidation to the edge-sharing species.

A puzzling artifact of these reactions is the formation of Mo≡^{4}MoCl$_4$(μ-dppm)$_2$ and β-Mo≡^{4}MoCl$_4$(μ-dppe)$_2$. In both cases, the crude precipitate and the crystals were found to contain 16–24% of the dimolybdenum species and 76–84% of the mixed-metal species. It should be noted that the purity of the starting material was established using both ^{1}H NMR and ^{31}P{^{1}H} NMR spectroscopy and was found to contain greater than 98% Mo≡^{4}WCl$_4$(PMePh$_2$)$_4$. Preliminary results indicate the amount of dimolybdenum product formed is dependent on the reaction time and temperature. Without further investigation one can only speculate as to the factors which lead to and control the amount of the dimolybdenum complex formed.

Structure and Bonding. The initial investigations of bridged-heteronuclear complexes by McCarley et al.[4] and Cotton et al.[5] revealed shorter than expected Mo≡^{4}W bond distances in Mo≡^{4}W(O$_2$CCMe$_3$)$_4$ and Mo≡^{4}W(mhp)$_4$ suggesting that there might be some special stability. However, in investigations of unbridged Mo≡^{4}WCl$_4$P$_4$ type complexes, Morris and Luck[8] did not find short Mo≡^{4}W bonds; in fact they found distances which are slightly longer than the mean of the Mo≡^{4}Mo and the W≡^{4}W bonds. Comparisons between these two systems indicated that the bridging ligands in the initial work might contribute to the shortness of the metal–metal bond.[4]

In order to investigate more thoroughly the effects of bridging ligands in these systems, several Mo≡^{4}WCl$_4$(L-L)$_2$ type complexes have been synthesized and characterized. The structural

(17) Cotton, F. A.; Luck, R. L.; James, C. A. To be published elsewhere with other related compounds.
(18) Cole, N. F.; Derringer, D. R.; Fiore, E. A.; Knoechel, D. J.; Schmitt, R. D.; Smith, T. J. *Inorg. Chem.* **1985**, *24*, 1978.
(19) Best, S. A.; Smith, T. J.; Walton, R. A. *Inorg. Chem.* **1978**, *17*, 99.
(20) Canich, J. M.; Cotton, F. A. *Inorg. Chim. Acta* **1988**, *142*, 69.
(21) Canich, J. M.; Cotton, F. A.; Luck, R. L.; Vidyasagar, K. *Organometallics* **1991**, *10*, 352.

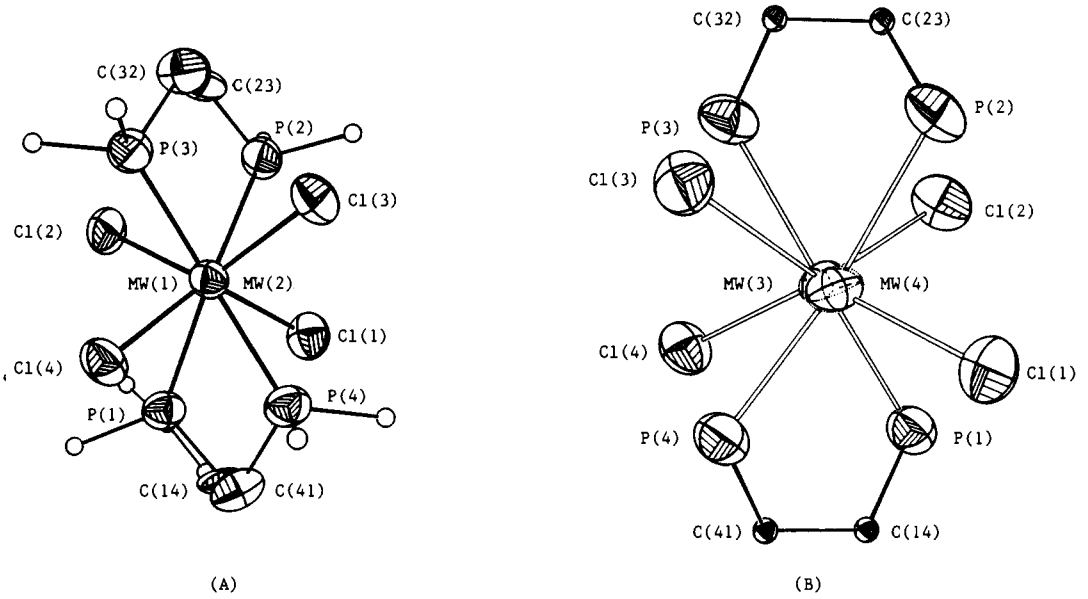

Figure 3. ORTEP drawings of β-Mo$\frac{4}{}$WCl$_4$(μ-dppe)$_2$ showing the torsional angles of the major (A) and minor (B) orientations (phenyl rings of dppe omitted). Thermal ellipsoids, except carbons, are drawn at 50% probability. The carbon atoms are shown as arbitrarily sized uniform circles.

Table VI. Positional and Thermal Parameters for Non-Hydrogen Atoms of α-Mo$\frac{4}{}$WCl$_4$(dmpe)$_2$ (**4**)

atom	x	y	z	B,[a] Å^2
MW(1)[b]	0.0501 (2)	0.0102 (1)	0.4302 (2)	1.59 (4)
Cl(1)	0.294 (1)	−0.0204 (8)	0.5055 (9)	2.5 (2)
Cl(2)	0.111 (1)	0.1492 (7)	0.410 (1)	2.2 (2)
Cl(11)	0.511 (2)	0.2666 (9)	−0.001 (1)	4.6 (3)
Cl(12)	0.371 (1)	0.4852 (9)	0.690 (1)	4.2 (3)
Cl(13)	0.447 (1)	0.6883 (9)	0.740 (1)	4.1 (3)
Cl(14)	0.238 (1)	0.335 (1)	0.612 (1)	4.3 (3)
P(1)	0.003 (1)	−0.1212 (7)	0.3310 (9)	2.3 (2)
P(2)	−0.159 (1)	0.0325 (7)	0.245 (1)	2.1 (3)
C(1)	0.274 (5)	0.443 (3)	0.314 (5)	4 (1)
C(2)	0.186 (4)	0.357 (3)	0.259 (4)	2.8 (9)
C(3)	0.287 (5)	0.616 (3)	0.262 (5)	3 (1)
C(4)	0.064 (4)	0.714 (3)	0.910 (3)	3.2 (9)
C(5)	0.077 (4)	0.628 (2)	0.709 (3)	2.0 (8)
C(6)	0.111 (5)	0.555 (4)	0.391 (4)	5 (1)
C(11)	0.355 (4)	0.392 (3)	0.753 (3)	2.5 (9)
C(12)	0.522 (6)	0.650 (4)	0.903 (3)	6 (2)

[a] Anisotropically refined atoms are given in the form of the equivalent isotropic displacement parameter defined as $^1/_3[a^2a^{*2}B_{11} + b^2b^{*2}B_{22} + c^2c^{*2}B_{33} + 2ab(\cos\gamma)a^*b^*B_{12} + 2ac(\cos\beta)a^*c^*B_{13} + 2bc(\cos\alpha)b^*c^*B_{23}]$. [b] Hybrid metal atom composed of 50.0% Mo and 50.0% W.

Table VII. Complete Bond Lengths (Å) for α-Mo$\frac{4}{}$WCl$_4$(dmpe)$_2$ (**4**)[a]

MW(1)[b]–MW(1)	2.234 (4)	Cl(14)–C(11)	1.88 (4)
MW(1)–Cl(1)	2.41 (1)	P(1)–C(2)	1.89 (4)
MW(1)–Cl(2)	2.45 (1)	P(1)–C(4)	1.80 (4)
MW(1)–P(1)	2.44 (1)	P(1)–C(5)	1.83 (5)
MW(1)–P(2)	2.43 (1)	P(2)–C(1)	1.89 (5)
Cl(11)–C(12)	1.90 (6)	P(2)–C(3)	1.91 (5)
Cl(12)–C(11)	1.75 (5)	P(2)–C(6)	1.84 (5)
Cl(13)–C(12)	1.84 (4)	C(1)–C(2)	1.69 (7)

[a] Numbers in parentheses are estimated standard deviations in the least significant digit. [b] Hybrid metal atom composed of 50.0% Mo and 50.0% W.

characterizations of compounds **1**–**3** are the first for quadruply bonded mixed-metal complexes with bridging bidentate phosphine ligands. The observed metal–metal bond lengths fail to show any evidence of "special shortness" relative to their quadruply bonded dimolybdenum and ditungsten analogs.

In order to easily compare the relative metal–metal bond lengths of complexes **1**–**4** with other heteronuclear complexes as well as their homonuclear analogs, the formal shortness ratio (FSR)[22] has been calculated for several of these complexes using eq 1,

Table VIII. Complete Bond Angles (deg) for α-Mo$\frac{4}{}$WCl$_4$(dmpe)$_2$ (**4**)[a]

MW(1)[b]–MW(1)–Cl(1)	115.0 (3)	C(2)–P(1)–C(4)	102 (2)
MW(1)–MW(1)–Cl(2)	114.7 (3)	C(2)–P(1)–C(5)	103 (2)
MW(1)–MW(1)–P(1)	97.2 (3)	C(4)–P(1)–C(5)	99 (2)
MW(1)–MW(1)–P(2)	97.9 (3)	MW(1)–P(2)–C(1)	116 (2)
Cl(1)–MW(1)–Cl(2)	87.7 (4)	MW(1)–P(2)–C(3)	122 (1)
Cl(1)–MW(1)–P(1)	88.7 (4)	MW(1)–P(2)–C(6)	109 (1)
Cl(1)–MW(1)–P(2)	145.6 (4)	C(1)–P(2)–C(3)	103 (2)
Cl(2)–MW(1)–P(1)	146.2 (4)	C(1)–P(2)–C(6)	101 (3)
Cl(2)–MW(1)–P(2)	87.3 (4)	C(3)–P(2)–C(6)	102 (3)
P(1)–MW(1)–P(2)	77.0 (4)	P(2)–C(1)–C(2)	111 (3)
MW(1)–P(1)–C(2)	115 (1)	P(1)–C(2)–C(1)	110 (3)
MW(1)–P(1)–C(4)	125 (1)	Cl(12)–C(11)–Cl(14)	103 (2)
MW(1)–P(1)–C(5)	110 (1)	Cl(11)–C(12)–Cl(13)	104 (3)

[a] Numbers in parentheses are estimated standard deviations in the least significant digit. [b] Hybrid metal atom composed of 50.0% Mo and 50.0% W.

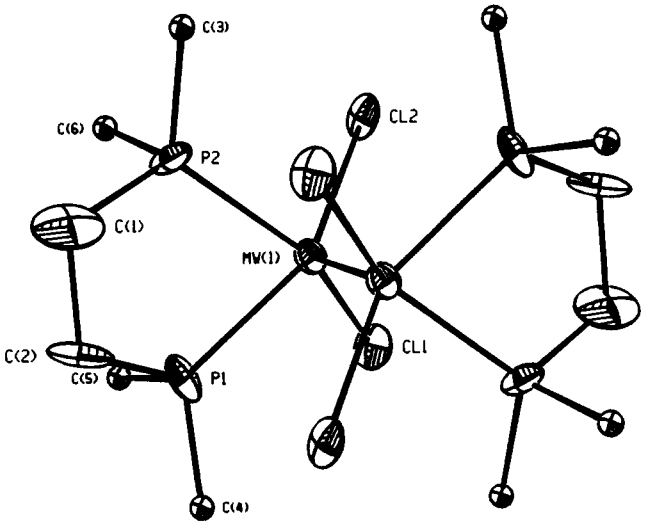

Figure 4. ORTEP drawing of α-Mo$\frac{4}{}$WCl$_4$(dmpe)$_2$. Thermal ellipsoids, except terminal carbons, are drawn at 50% probability. The terminal carbon atoms are shown as arbitrarily sized uniform circles.

(22) Cotton, F. A.; Koch, S.; Millar, M. *J. Am. Chem. Soc.* **1977**, *99*, 7372.

Table IX. Comparison of Important Dimensions (Å, deg) between M≡M′Cl$_4$(L-L)$_2$ Complexes, Where L-L = dppm and dppe

	Mo≡WCl$_4$(L-L)$_2$		Mo≡MoCl$_4$(L-L)$_2$		W≡WCl$_4$(L-L)$_2$	
bond or angle	dppm	dppe	dppm[26]	dppe[27]	dppm[20]	dppe[24]
M–M′	2.2110 (7)	2.243 (1)	2.138 (1)	2.2183 (3)	2.269 (1)	2.314 (1)
M–P(av)	2.5715 (2)	2.554 (5)	2.585 (1)	2.579 (8)	2.560 (2)	2.534 (5)
M–Cl(av)	2.383 (2)	2.384 (4)	2.394 (1)	2.385 (7)	2.376 (2)	2.372 (4)
Cl–M–Cl(av)	143.15 (8)	135.3 (1)	146.18 (5)	135.3 (3)	143.17 (9)	135.0 (2)
P–M–P(av)	163.46 (7)	165.6 (2)	161.79 (4)	165.6 (3)	167.00 (8)	166.5 (2)
M–M–P(av)	96.32 (5)	97.01 (1)	98.57 (4)	97.1 (2)	95.79 (6)	96.6 (1)
M–M–Cl(av)	108.59 (6)	112.3 (1)	106.86 (4)	112.3 (2)	107.88 (7)	112.5 (1)
torsional	15.25	58.8	0	30.5	17.25	31.3

where D_{AB} is the metal–metal bond distance and R_A and R_B are the single-bond metallic radii of the metals.[23]

$$\text{FRS} = \frac{D_{AB}}{R_A + R_B} \qquad (1)$$

The calculated FSR's for **1**–**4** range from 0.843 for Mo≡WCl$_4$(μ-dmpm)$_2$ to 0.863 for β-Mo≡WCl$_4$(μ-dppe)$_2$ and α-Mo≡WCl$_4$(dmpe)$_2$. In comparison, the FSR's for their dimolybdenum analogs range from 0.823 to 0.843, while those for the ditungsten analogs range from 0.870 to 0.887. The FSR's for Mo≡W(O$_2$CCMe$_3$)$_4$ and Mo≡W(mhp)$_4$ are 0.800 and 0.804, respectively. These bonds are indeed formally shorter than bonds in **1**–**4** and Mo≡WCl$_4$P$_4$ type complexes, where the FSR's are ca. 0.850. In comparison to the homonuclear complexes, Mo≡Mo(O$_2$CCMe$_3$)$_4$ (FSR = 0.807),[4] W≡W(O$_2$CCF$_3$)$_4$ (FSR = 0.847),[24] Mo≡Mo(mhp)$_4$ (FSR = 0.797),[5] and W≡W(mhp)$_4$ (FSR = 0.826),[5] it is apparent that only the metal–metal bond in Mo≡W(O$_2$CCMe$_3$)$_4$ is formally shorter than its dimolybdenum analog.

There are two factors which may tend to make real or apparent changes in the observed metal–metal bond lengths in complexes **1** and **2**. These are the torsional angles about the M–M′ vectors and the solid solution nature of the crystals. The effect of the torsional angle is well understood and may only tend to lengthen the bond distance.[25] In contrast, the effect the solid solution has on the metal–metal bond length is not well understood, and it must always be kept in mind that, in structures such as those of **1** and **2**, one obtains from the X-ray diffraction data an electron density distribution that is a convolution for two different species at each point in space. Therefore, it does not allow one to obtain molecular structure parameters (bond lengths, angles) of the same precision as one would, other things being equal, for a crystal in which all sites are occupied by truly identical chemical entities. The bond lengths and angles obtained are not exactly those of either species in the crystal, and the estimated standard deviations (esd's) given by the least squares are not strictly applicable. As a result of the preceding considerations, it is necessary to be cautious about comparing differences between structural data when some or all are derived from crystals showing this type of disorder.

The crystals of **1**–**4** all also exhibit the usual type of disorder (i.e., random arrangement of the M–M′ vector) for heteronuclear systems. This arrangement causes the metal to ligand bond distances to be an average of the Mo–L and W–L (L = Cl or P) distances.[1] Because of this averaging, only the metal–metal bond lengths and overall conformations of **1**–**4** may be determined precisely. The important structural dimensions for **1** and **2** and their homonuclear homologs have been tabulated in Table IX, while similar dimensions for **3** and **4** have been tabulated in Table X. All of these complexes show the expected general structural characteristics. The characteristics specific for each complex and the relationships between them will be explored in the following paragraphs.

Table X. Comparison of Important Dimensions (Å, deg) between M≡M′Cl$_4$(L-L)$_2$ Complexes, Where L-L = dmpm and dmpe

	Mo≡Cl$_4$(L-L)$_2$		Mo≡MoCl$_4$(L-L)$_2$	W≡WCl$_4$(L-L)$_2$
bond or angle	dmpm	dmpe	dmpm[36]	dmpe[28]
M–M′	2.193 (2)	2.243 (1)	2.134 (4)	2.287 (2)
M–P(av)	2.58 (1)	2.44 (1)	2.477 (4)	2.448 (2)
M–Cl(av)	2.35 (1)	2.43 (1)	2.477 (4)	2.425 (2)
Cl–M–Cl(av)	150.0 (5)	87.4 (4)	153.3 (2)	86.38 (8)
P–M–P(av)	162.2 (5)	77.0 (4)	153.3 (2)	77.95 (7)
M–M–P(av)	98.9 (4)	97.5 (3)	103.4 (1)	96.38 (5)
M–M–Cl(av)	105.0 (5)	114.9 (3)	103.4 (1)	116.08 (1)
torsional	≈0	0	0	0

Compound 1. The structural characterization of **1** revealed little that was unexpected. The observed average torsional angle of 15.25°, shown in Figure 1, is one of the more interesting structural features. The magnitude of the torsional angle is comparable to that observed in W$_2$Cl$_4$(μ-dppm)$_2$ (17.25°)[20] but is significantly different from that observed in Mo≡MoCl$_4$(μ-dppm)$_2$ (0°).[26] The twisting of the metal–metal vector causes a decrease in the δ overlap as a function of cos 2θ, where θ is the torsional angle. Compound **1** does not deviate from the expected behavior. There is an increase in the metal–metal distance (0.02 Å) relative to **3**, which has a torsional angle of 0°.

This twisted conformation is of special interest in light of the solid solution nature of the crystal. The crystals of **1** are found to contain approximately 84% Mo≡WCl$_4$(μ-dppm)$_2$ and 16% Mo≡MoCl$_4$(μ-dppm)$_2$. These values were obtained from the least-squares calculations and were confirmed using ^{31}P{^{1}H} NMR spectroscopy. The refinement of this structure failed to indicate the presence of the ligand atom positions for an untwisted dimolybdenum molecule implying that Mo≡MoCl$_4$(μ-dppm)$_2$ has adopted the twisted conformation of the host lattice, Mo≡WCl$_4$(μ-dppm)$_2$, in this solid solution.

Compound 2. This compound is also similar to its dimolybdenum and ditungsten counterparts.[24,27] The M–M′ vector is found to be disordered in two orientations which are orthogonal to one another. The population of the major orientation is 93%, while that of the minor orientation is 7%. In comparison, β-Mo≡MoCl$_4$(μ-dppe)$_2$[27] has a 87:13 distribution, while β-W≡WCl$_4$(μ-dppe)$_2$[24] has a 93:7 distribution. The observed average torsional angles of 58.8° for the major orientation and 62.32° for the minor orientation, shown in Figure 3, are not only the largest yet observed in a heteronuclear complex but the largest observed for a quadruply bonded complex containing dppe. The observed torsional angles for the homonuclear complexes are both on the order of 30°. Because δ bond overlap is a function of the cosine of twice the torsional angle, the net bonding effect of a 60° torsional angle is the same as that of a 30° angle.

Like those of compound **1**, crystals of **2** exhibit characteristics of a solid solution. The crystals of **2** were found to contain 76%

(23) Pauling, L. C. *The Nature of The Chemical Bond*; Cornell University Press: Ithaca, NY, 1960.
(24) Cotton, F. A.; Felthouse, T. R. *Inorg. Chem.* **1981**, *20*, 3880.
(25) Campbell, F. L.; Cotton, F. A.; Powell, G. L. *Inorg. Chem.* **1985**, *24*, 177.
(26) Abbott, E. H.; Bose, K. S.; Cotton, F. A.; Hall, W. T.; Sekutowski, J. C. *Inorg. Chem.* **1978**, *17*, 3240.
(27) Agaskar, P. A.; Cotton, F. A. *Inorg. Chem.* **1984**, *23*, 3383.

Table XI. Spectroscopic Data for Complexes **1–5**

complex	$^{31}P\{^1H\}$ NMR resonances, δ	^1H NMR resonances, δ	UV–vis abs, nm
Mo$\equiv$WCl$_4$(μ-dppm)$_2$ (**1**)	1.8 (m, 2P, P–Mo), 42.1 (m, 2P, P–W)	7.6–6.9 (m, 40H, *Ph*P–M, M = Mo, W), 4.65 (m, 4H, *CH*$_2$P–M, M = Mo, W)	675
β-Mo$\equiv$WCl$_4$(μ-dppe)$_2$ (**2**)	30.6 (vt, 2P, P–Mo), 56.0 (vt, 2P, P–W) ($J(P_W–P_{Mo}) \approx 20$ Hz)	8.0–7.0 (m, 40H, *Ph*P–M, M = Mo, W), 3.40 (m, 4H, *CH*$_2$P–Mo), 3.77 (m, 4H, *CH*$_2$P–W)	810, 475
α-Mo$\equiv$WCl$_4$(dppe)$_2$ (**5**)		8.0–6.4 (m, 40H, *Ph*P–M, M = Mo, W), 4.67, 3.27 (m, 4H, *CH*$_2$P–Mo), 5.02, 3.50 (m, 4H, *CH*$_2$P–W)	740
Mo$\equiv$WCl$_4$(μ-dmpm)$_2$ (**3**)	−14.5 (m, 2P, P–Mo), 24.1 (m, 2P, P–W)	3.4 (m, 4H, *CH*$_2$P–M, M = Mo, W), 1.34 (m, 6H, *CH*$_3$P–Mo), 1.34 (m, 6H, *CH*$_3$P–W)	628
α-Mo$\equiv$WCl$_4$(dmpe)$_2$ (**4**)	23.7 (dd, 2P, P–Mo), 47.8 (dd, 2P, P–W) ($^1J_{P-W}$ = 300 Hz; $^2J_{P-W}$ = 100 Hz; $J(P_W–P_{Mo}) \approx 28$, 24 Hz)	1.62 (m, 6H, *CH*$_3$P–Mo), 1.83 (m, 6H, *CH*$_3$P–W), 3.14, 1.77 (m, 4H, *CH*$_2$P–Mo), 3.48, 2.13 (m, 4H, *CH*$_2$P–W)	740

β-Mo$\equiv$WCl$_4$(μ-dppe)$_2$ and 24% β-Mo$\equiv$MoCl$_4$(μ-dppe)$_2$. Again, these values were obtained from the least-squares calculations and were confirmed using $^{31}P\{^1H\}$ NMR spectroscopy. The refinement of this structure failed to indicate the presence of ligand atom positions for a dimolybdenum molecule with a different torsional angle. This indicates that β-Mo$\equiv$MoCl$_4$(μ-dppe)$_2$ has adopted the conformation of the host lattice, β-Mo$\equiv$WCl$_4$(μ-dppe)$_2$, in this solid solution.

Compound 3. The metal–metal bond length in **3** is somewhat shorter than that observed in **1** [2.193 (2) vs 2.211 (1) Å] and is formally shorter (FSR = 0.843) than that in unbridged Mo$\equiv$WCl$_4$P$_4$ type complexes (FSR = 0.850).[8] This shortening is due primarily to the eclipsed conformation of this molecule causing an increase in the δ orbital overlap relative to that of **1**. The increased basicity and smaller size of dmpm relative to dppm may also contribute to the decrease in the metal–metal distance. A similar effect has been observed in the structures of Mo$\equiv$MoCl$_4$(μ-dppm)$_2$ and Mo$\equiv$MoCl$_4$(μ-dmpm)$_2$.

Compound 4. The structure of α-Mo$\equiv$WCl$_4$(dmpe)$_2$ is of particular interest because it is the first example of heteronuclear quadruply bonded complex in which diphosphine ligands are chelated instead of bridging. It also provides one of the first examples of a Mo$\equiv$WCl$_4$P$_4$ type molecule in which the MX$_2$P$_2$ unit has a cis instead of trans arrangement. This results in a Mo–W bond length of 2.243 (1) Å, which is significantly longer than in related Mo$\equiv$WCl$_4$P$_4$ type complexes.

There are also differences in the M–Cl and M–P bond lengths in comparison to Mo$\equiv$WCl$_4$(PMe$_3$)$_4$.[8] The M–Cl distances, trans to Cl, are 2.395 (2) and 2.406 (2) Å in Mo$\equiv$WCl$_4$(PMe$_3$)$_4$, while the M–Cl distances, trans to P, in **4** are 2.41 (1) and 2.45 (2) Å. Similarly, the M–P distances, trans to P, in Mo$\equiv$WCl$_4$(PMe$_3$)$_4$ are 2.532 (2) and 2.539 (2) Å, while the M–P distances, trans to Cl, in **4** are 2.44 (1) and 2.43 (1) Å. These differences in M–Cl (0.03 (1) Å) and M–P (0.10 (1) Å) distances seem to be manifestations of structural trans influence similar to those found in α-W$\equiv$WCl$_4$(dmpe)$_2$ and other square-planar complexes.[28]

Electronic Spectra. The solution spectra of all complexes were recorded in THF or acetone as dissolution in CH_2Cl_2 or other chlorinated solvents resulted in the formation of M$_2$X$_6$(L-L)$_2$ species. In the visible region of their electronic spectra, all complexes display a prominent absorption band that is assigned to the $\delta^2 \rightarrow (\delta\delta^*)$ transition. This band is substantially red shifted in β-Mo$\equiv$WCl$_4$(μ-dppe)$_2$ (810 nm) relative to the position for α-Mo$\equiv$WCl$_4$(dppe)$_2$ (740 nm). A similar shift has been seen for the homonuclear dimolybdenum complexes.[27,29] The red shift is expected since the α isomers are eclipsed whereas the β isomers have appreciable angles of twist, which weaken the δ bonding.[25] One may also note that the band is shifted to higher energies for

Table XII. Comparison of Electronic Absorption Data for M$\equiv$M′Cl$_4$(L-L)$_2$

	$\delta^2 \rightarrow (\delta\delta^*)$ abs band, nm		
L-L	Mo$\equiv$WCl$_4$(L-L)$_2$	Mo$\equiv$MoCl$_4$(L-L)$_2$	W$\equiv$WCl$_4$(L-L)$_2$
β-dppm	665	634[18]	737[20]
β-dppe	810	740[27]	850[37]
α-dppe	740	680[27]	795[37]
β-dmpm	628	604[36]	668[15]
α-dmpe	720	655[37]	755[37]

Mo$\equiv$WCl$_4$(μ-dmpm)$_2$ (628 nm) and α-Mo$\equiv$WCl$_4$(dmpe)$_2$ (720 nm) relative to Mo$\equiv$WCl$_4$(μ-dppm)$_2$ (665 nm) and α-Mo$\equiv$WCl$_4$(dppe)$_2$ (740 nm). This shift is attributed to the increased basicity of the phosphine and has also been observed in the homologous species. The positions of all absorptions for complexes **1–4** are listed in Table XI, while a comparison of the $\delta^2 \rightarrow (\delta\delta^*)$ transition with their homonuclear counterparts is given in Table XII.

$^{31}P\{^1H\}$ NMR Analysis. The identities of these heteronuclear complexes are readily established by their distinctive $^{31}P\{^1H\}$ NMR spectra. The spectra of **1–4** are complex as expected for AA′BB′X spin systems. Figure 5 shows the spectrum of **1**, which is similar to the spectrum of **3**. Complexes **2** and **4** have geometries different from those of **1** and **3** and therefore, exhibit different complex patterns. These patterns are shown in Figures 6 and 7. Approximate P–P coupling constants for **2** and **4** may be obtained from the spectra and are listed in Table XI. Complex **2** produces a splitting pattern which is roughly a virtual triplet (vt) with a $J(P_W–P_{Mo})$ value of approximately 20 Hz. Complex **4** produces a splitting pattern which is roughly a doublet of doublets, and two J(P–P)'s may be obtained from this spectrum. These coupling constants are approximately 24 and 28 Hz. Attempts to calculate more accurate coupling constants and to simulate spectra of complexes **1–4** resulted only in first-order approximations.

The $^{31}P\{^1H\}$ NMR chemical shift data for **1–4** and the analogous dimolybdenum and ditungsten complexes have been listed in Table XIII. No $^{31}P\{^1H\}$ NMR spectrum was obtained for **5** as the complex was extremely insolubility in all common solvents.

The magnitude of the chemical shift differences between the phosphorus ligands on the different metals [δ(P–W) − δ(P–Mo) = 40.2–24.1 ppm] is consistent with differences observed for other Mo$\equiv$W systems.[8] A possible explanation for this is the transfer of electronic density from tungsten to molybdenum in the heteronuclear species and would result in a difference in effective charge between the two metal atoms. The chemical shifts of the phosporus atoms would then be attributed to either the resulting paramagnetic effects or simple diamagnetic screening considerations or a combination of these two effects.[30] In all cases, the downfield pattern has been assigned to the phosphorus atoms bound to tungsten and the upfield pattern has been assigned to the phosphorus atoms bound to molybdenum. The assignments were made on the basis of $^{31}P–^{183}W$ coupling observed in the case

(28) Cotton, F. A.; Extine, M. W.; Felthouse, T. R.; Kolthammer, B. W. S.; Lay, D. G. *J. Am. Chem. Soc.* **1981**, *103*, 4040.
(29) Agaskar, P. A.; Cotton, F. A. *Inorg. Chem.* **1986**, *25*, 15.
(30) Carlin, R. T.; McCarley, R. E. *Inorg. Chem.* **1989**, *28*, 280.

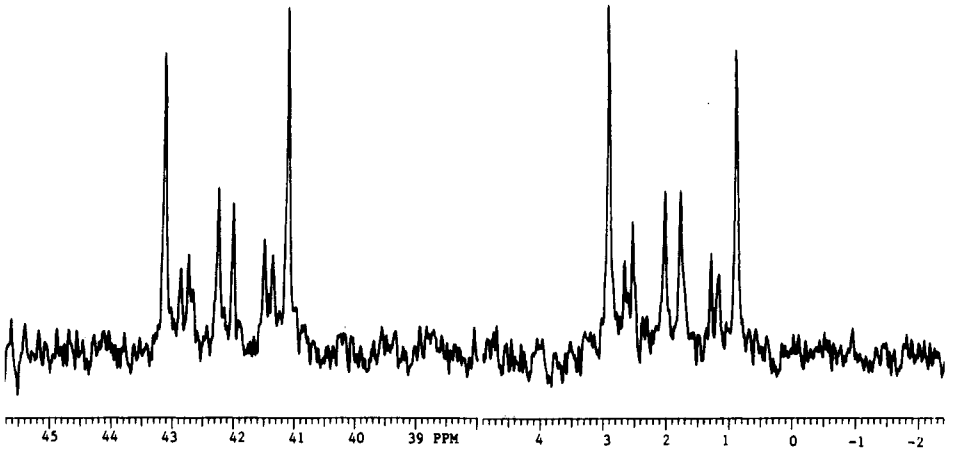

Figure 5. $^{31}P\{^1H\}$ NMR spectrum of Mo≡$WCl_4(\mu\text{-dppm})_2$. The analysis is presented in Results and Discussion.

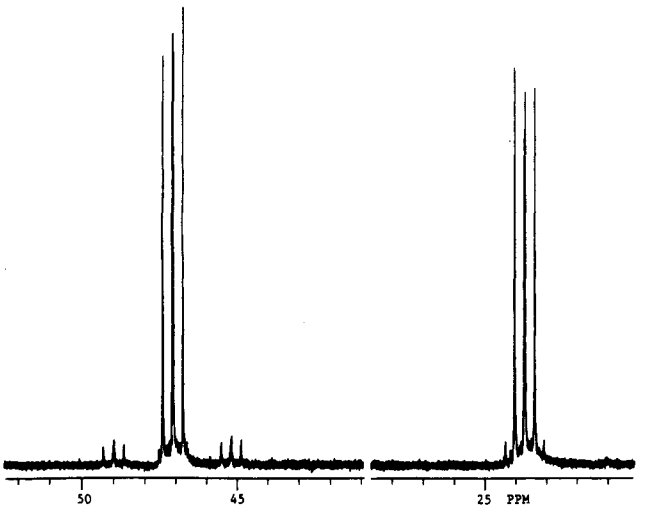

Figure 6. $^{31}P\{^1H\}$ NMR spectrum of α-Mo≡$WCl_4(dmpe)_2$. The analysis is presented in Result and Discussion.

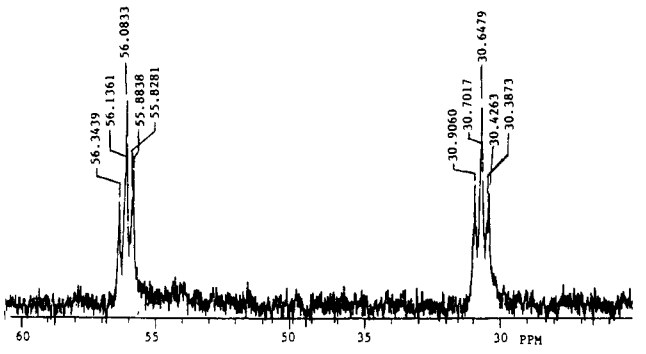

Figure 7. $^{31}P\{^1H\}$ NMR spectrum of β-Mo≡$WCl_4(\mu\text{-dppe})_2$. The analysis is presented in Results and Discussion.

of **4** and in comparison to positions of resonances in similar heteronuclear complexes for **1–3**.[2,8] The absolute differences between such chemical shifts for analogous homonuclear complexes with the same bidentate phosphines are also listed in Table XIII.

The spectrum of complex **4** is of particular interest as it provides an opportunity to examine the characteristics of cis diphosphines on heteronuclear complexes. The most notable features in the spectrum of **4** are the prominence of the ^{183}W satellites and its simplicity, relative to those of **1–3**. The magnitude of the $^1J(^{31}P-^{183}W)$ coupling (320 Hz) is significantly larger than that observed for trans phosphines (266–275 Hz), as one might expect. The $^2J(^{31}P-^{183}W)$ coupling (100 Hz) is also significantly larger than that observed in systems with trans phosphines (≈47 Hz).[8]

Table XIII. Comparison of $^{31}P\{^1H\}$ NMR Chemical Shifts for M≡$M'Cl_4(L\text{-}L)_2$ Complexes

	Mo≡$WCl_4(L\text{-}L)_2$			Mo≡$MoCl_4(L\text{-}L)_2$ and W≡$WCl_4(L\text{-}L)_2$		
L-L	δ(P–Mo)	δ(P–W)	δ(P–W) – δ(P–Mo)	δ(P–Mo)	δ(P–W)	δ(P–W) – δ(P–Mo)
β-dppm	1.88	42.10	40.22	16.04[37]	18.14[37]	2.10
β-dppe	30.6	56.0	25.4	38.2[37]	40.93[37]	2.73
β-dmpm	−14.48	24.05	38.53	0.77[36]		
α-dmpe	23.7	47.8	24.1	31.5[37]	32.98[38]	1.48

It should be noted that all spectra were recorded in CD_2Cl_2 or $CDCl_3$ at temperatures below −40 °C. These complexes all undergo oxidation in chlorinated solvents at ambient temperatures.

^1H NMR Analysis. The ^1H NMR spectra of **1–5** have several interesting features which have not been previously observed. In all cases, these complexes have methylene or ethylene protons located in positions where they are affected by the diamagnetic anisotropy of the quadruple bond. In addition, one is able to distinguish two separate resonances for each type of protons due to the same effects that cause the differences in the ^{31}P chemical shift values. The downfield resonance of each pair is due to the protons of the phosphines bound to the tungsten while the upfield resonance is due to the protons of the phosphines bound to the molybdenum. The resonances appear as complex multiplets, and the positions of these multiplets for each type of proton have been listed in Table XI. It should be noted that all spectra were recorded in CD_2Cl_2 or $CDCl_3$ at temperatures below −40 °C. These complexes all undergo oxidation in chlorinated solvents at ambient temperatures.

Diamagnetic Anisotropy of the Mo≡W Bond. The chemical shift difference observed in the ^1H NMR spectra for certain protons and their positions as calculated from the X-ray crystal structure data[31] for complexes **1–4** can be used to estimate the diamagnetic anisotropy of the molybdenum–tungsten quadruple bond. For complexes **1–4** the methods and reference frame of Cotton et al.[32] have been used to estimate $\Delta\chi$ using eq 2.

$$\Delta\delta = \frac{\Delta\chi}{4\pi}\left[\frac{1-3\cos^2\theta}{3r^3}\right] = \frac{\Delta\chi}{4\pi}G \qquad (2)$$

Here $\Delta\chi$ is the change in the chemical shift of the proton relative to the free ligand, r is the distance of the test nucleus from the center of the Mo≡W bond, and θ is the angle between the r vector and the Mo–W axis. Table XIV contains the observed $\Delta\delta$'s, G factors, and the calculated $\Delta\chi$ values for **1–4**. Estimations of $\Delta\chi$ made using this method contain ambiguities concerning

(31) The C–H distances are 1.08 Å, and the C–C–H angles are 109°.
(32) Chen, J. D.; Cotton, F. A.; Falvello, L. R. *J. Am. Chem. Soc.* **1990**, *112*, 1076.

Table XIV. Diamagnetic Anisotropy of Mo≡W for Complexes **1–4**

L-L	G_{av}[a]	$\Delta\delta$, ppm	$\Delta\chi$[b]
β-dppe	3.24	1.58	−6120
β-dppm	4.96	1.75	−4431
β-dmpm	5.11	2.0	−4915
α-dmpe H^P	5.34	1.96	−4615
α-dmpe H^D	1.53	0.65	−5327

[a] Units in $\times 10^{-27}$ m^{-3}; $G = (1 - 3\cos^2\theta)/3r^3$. [b] Units in $\times 10^{-36}$ m^3 molecule^{-1}.

Table XV. Chemical Shift Values and Geometric Factors for Proximal and Distal Protons of α-Mo≡$WCl_4(dmpe)_2$ (**4**)

proton	δ, ppm	$G'_\perp$[a]	$G''_\perp$[a]
H_1^D	3.14	2.52	−4.57
H_1^P	1.77	3.59	−8.79
H_1^P	3.48	4.22	−9.70
H_1^D	2.13	2.49	−4.61

[a] Units in $\times 10^{-27}$ m^{-3}; $G = (1 - 3\cos^2\theta)/3r^3$. Superscripts D and P denote distal and proximal, respectively.

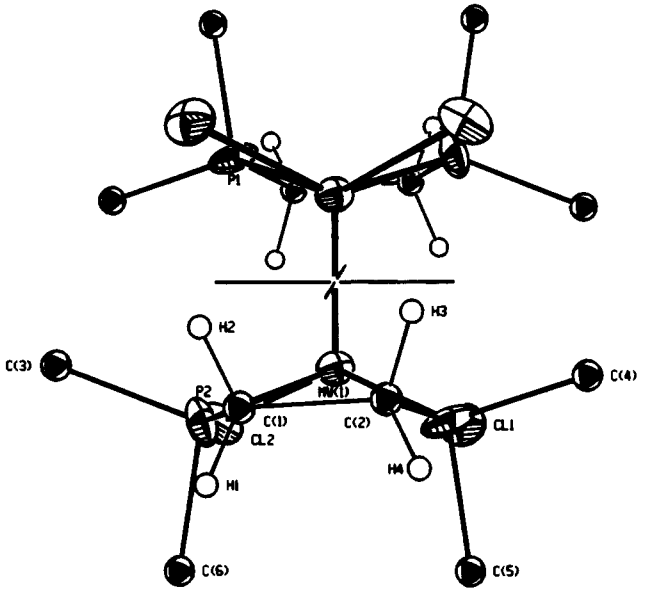

Figure 8. ORTEP drawing showing the positions of the proximal, H2 and H3, and distal, H1 and H2, protons in α-Mo≡$WCl_4(dmpe)_2$. Thermal ellipsoids, except terminal carbons, are drawn at 50% probability. The carbon atoms are shown as arbitrarily sized uniform circles.

the portion of $\Delta\delta$ which is actually due to $\Delta\chi$ and the portions which may be due to ring current effects of nearby phenyl rings or inductive effects resulting from the phosphorus binding to the metal center. Using the values of $\Delta\chi$ for the five complexes, an average value of -5082×10^{-36} m^3 molecule^{-1} is obtained for the diamagnetic anisotropy of the Mo≡W bond. In comparison, an average value of -6500×10^{-36} m^3 molecule^{-1} has been reported for the Mo≡Mo bond and a value of -3000×10^{-36} m^3 molecule^{-1} has been estimated for the W≡W bond.[33] It should be noted that the value for the ditungsten complex seems to be unrealistically low compared to the dimolybdenum systems and preliminary calculations in this laboratory indicate the anisotropy of the W≡W bond to be slightly larger than in the dimolybdenum systems.

Complex **4** has two distinct types of protons as shown in Figure 8 and offers an opportunity to estimate $\Delta\chi$ using the method of Cotton and Kitagawa[34] by employing eq 3.

$$\Delta\delta_{distal} - \Delta\delta_{proximal} = \frac{(\chi_\parallel - \chi'_\perp)(G'_{distal} - G'_{proximal})}{4\pi} + \frac{(\chi_\parallel - \chi''_\perp)(G''_{distal} - G''_{proximal})}{4\pi} \quad (3)$$

This method eliminates the ambiguity concerning the true magnitude of $\Delta\delta$ but is only applicable in cases where two sets of observed chemical shifts are available. Table XV contains the observed values for δ and calculated $G'_\perp$ and $G''_\perp$ factors for each of the four ethylene protons of α-Mo≡$WCl_4(dmpe)_2$. Using the parameters listed in Table XV and eq 3, one may calculate the diamagnetic anisotropy. The values for $(\chi_\parallel - \chi'_\perp)$ and $(\chi_\parallel - \chi''_\perp)$ were found to be -7700×10^{-36} m^3 molecule^{-1} and -5800×10^{-36} m^3 molecule^{-1}, respectively. Average values of -8670×10^{-36} m^3 molecule^{-1} for $(\chi_\parallel - \chi'_\perp)$ and -5890×10^{-36} m^3 molecule^{-1} for $(\chi_\parallel - \chi''_\perp)$ were reported for the series of α-$Mo_2Cl_4(L\text{-}L)_2$ complexes, where L-L = dppe, dpdt, and dbdbp.[34] One must be careful in comparing these data with those for α-Mo≡$WCl_4(dmpe)_2$ as all of dimolybdenum systems contain phenyl rings, which may also affect the chemical shift of the ethylene protons. The ring current effect of the phenyl groups is estimated to be ≈12% of the whole anisotropy. If these ring current effects are not taken into account, the dimolybdenum system would seem to have a significantly larger anisotropy. However, when this effect is taken into account it becomes apparent that the diamagnetic anisotropy of the Mo≡W and Mo≡Mo bonds are essentially equal.

It is well-known that heteronuclear organic bonds such as C=O and N=O have larger anisotropies than analogous homonuclear bonds C=C.[35] In light of this fact, one might have expected the Mo≡W bond to have a larger anisotropy than either the Mo≡Mo or W≡W bonds. Results indicate that there is litte difference in the anisotropies of the Mo≡W and Mo≡Mo or W≡W bonds.

Acknowledgment. We are grateful to Dr. Larry Falvello for assistance in X-ray crystallography, to Dr. Rudy Luck for instruction in synthetic inorganic chemistry, and to the National Science Foundation for support.

Supplementary Material Available: Full lists of bond distances, bond angles, torsional angles, hydrogen atom positional parameters, and anisotropic thermal parameters and numbered ORTEP projections including phenyl rings of dppm ligands (32 pages). Ordering information is given on any current masthead page.

(33) Fryzuk, M. D.; Kreiter, C. G.; Sheldrick, W. S. *Chem. Ber.* **1989**, *122*, 851.
(34) Cotton, F. A.; Kitagawa, S. *Polyhedron* **1988**, *7*, 1673.
(35) Harris, R. K. *Nuclear Magnetic Resonance Spectroscopy*; Longman: London, 1986.
(36) Cotton, F. A.; Falvello, L. R.; Harwood, W. S.; Powell, G. L.; Walton, R. A. *Inorg. Chem.* **1986**, *25*, 3949.
(37) Cotton, F. A.; Eglin, J. L.; James, C. A. To be published elsewhere with related compounds.
(38) Schrock, R. R.; Sturgeoff, L. G.; Sharp, P. R. *Inorg. Chem.* **1983**, *22*, 2801.